

# Application of the Stabilization Method to the $\pi^*$ Temporary Anion States of Benzene and Substituted Benzenes in Density Functional Theory

Hsiu-Yao Cheng\* and Chun-Chi Shih

Department of Chemistry, Tunghai University, Taichung 40704, Taiwan

Received: September 18, 2008; Revised Manuscript Received: December 5, 2008

The stabilization method is used in conjunction with Koopmans-based approximation to calculate the energies of  $\pi^*$  temporary anion states of a series of substituted benzenes in density functional theory. In this approach, the Koopmans expression is corrected due to the consideration of the integer discontinuities in the exact exchange-correlation potential. Stabilization is accomplished by varying the exponents of appropriate diffuse functions. The energies of  $\pi^*$  states are then identified by investigating the relationship between the resultant eigenvalues and scale parameter. Results indicate that this approach can yield an improvement in the predictions of the absolute energies of  $\pi^*$  states over other methods.

## 1. Introduction

The temporary or metastable anion state<sup>1</sup> plays an important role in the study of electron–molecule collision processes. It is also important in the study of chemical properties such as chemical reactivity, hardness, softness, electronegativity, non-linear optical activity, and the electronic couplings responsible for the high rates of electron transfer in donor–bridge–acceptor compounds.<sup>2–9</sup> The temporary anion can be observed as a sharp resonance in the electron scattering cross section by electron transmission spectroscopy (ETS).<sup>10,11</sup> The resonance phenomenon, which occurs when an incident particle has the right energy to be trapped by the target-particle potential, can be regarded as a discrete state embedded in a continuum. Since the temporary anion state lies energetically above the ground state of the neutral molecule, its electron affinity (EA) is negative.

The determination of negative EA is a challenging problem for theoretical methods, since the anion is unstable with respect to electron detachment. Any variational methods are likely to fail due to “variational collapse” to the neutral molecule plus a free electron for temporary anion states. In many applications, the EAs are computed via Koopmans’ theorem (KT)<sup>12</sup> using Kohn–Sham orbital energies. The EA is associated with the negative of the unoccupied molecular orbital energy. However, there is a special difficulty when using the density functional theory (DFT)<sup>13</sup> method as far as anions are concerned.<sup>1,14</sup> The KT approximation often underestimates the exact EAs due to a fundamental deficiency in the potentials of conventional continuum functional.

Recently, Tozer and co-workers have studied temporary anions in DFT via an alternative Koopmans-based (KB) approximation.<sup>14–19</sup> A simple correction to the Koopmans expression is highlighted on the basis of a consideration of the integer discontinuity ( $\Delta_{xc}$ ) in the exact exchange-correlation potential. The correction of the Koopmans value is approximately half the integer discontinuity

$$\frac{\Delta_{xc}}{2} \approx \varepsilon_{\text{HOMO}} + \text{IP} \quad (1)$$

where

$$\text{IP} = E_{N-1} - E_N \quad (2)$$

Here,  $\varepsilon_{\text{HOMO}}$  is the highest-occupied molecular orbital (HOMO) energy determined from a DFT calculation using a local exchange-correlation functional on the neutral system. IP is the vertical ionization potential of the neutral, and  $E_N$  and  $E_{N-1}$  are the total electronic energies of the neutral and cation, respectively. The correction  $\Delta_{xc}/2$  can eliminate the underestimation of the Koopmans expression for EAs. The applications by Tozer et al. have been shown to give improvement over other approaches for systems with large negative EAs. However, their studies are mainly for electron capture into the lowest unoccupied molecular orbital (LUMO) of a neutral, ground-state system.

For temporary anion states, the KT approximation may not generate definitive energies by adopting a basis set with more diffuse functions in finite basis set calculations. This is because the temporary anion states are prone to collapse onto continuum solutions, called orthogonalized discrete continuum (ODC)<sup>20–23</sup> solutions. The stabilization method proposed by Taylor and co-workers<sup>24–27</sup> can allow one to distinguish the temporary anion orbital solutions from the ODC solutions. Their method has been employed in conjunction with KT. The vertical attachment energies (AEs) are associated with the energies of the “stabilized” temporary anion states of the neutral molecules. The stabilized Koopmans’ theorem (SKT) method (i.e., the stabilization method coupled with KT) has been much more successful than KT alone in predicting relative energies of temporary anion states.<sup>28–30</sup>

So far, the stability of the resonance energies has not been systematically examined by using the DFT method. We notice that the SKT method is successful in predicting relative energies of higher virtual orbits. In addition, the KB approach differs from KT only by a correction term,  $\Delta_{xc}/2$ . Hence, it is vital to couple the aforementioned alternative KB approximation and the stabilization method via DFT method to study the temporary anion states. In the past, we have studied the  $\pi^*$  temporary anion states of benzene, fluorobenzene, phenol, and pyridine using

\* Corresponding author. Telephone: 011-886-4-23590248-102. Fax: 011-886-4-23590426. E-mail: hycheng@thu.edu.tw.

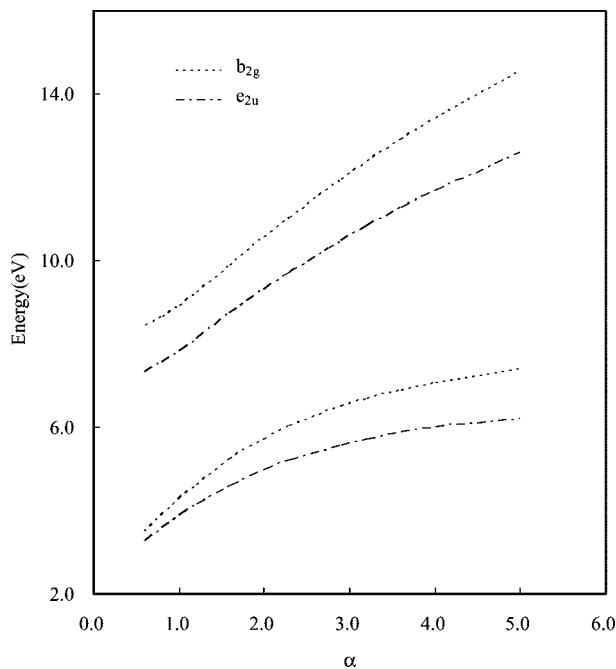


**Figure 1.** Energies of  $e_{2u}$  and  $b_{2g}$  virtual orbitals of benzene as a function of the scaling factor  $\alpha$  for a free electron in the absence of potentials using 6-31+G(d)+ $\alpha p_1$  basis set.

the stabilization method in conjunction with the  $X\alpha$  method<sup>28</sup> and KT approximation.<sup>29</sup> In this study, it is fitting for us to study a series of substituted benzenes via the stabilization method in conjunction with an alternative KB approximation (S-KB) in DFT. Finally, the results obtained from both S-KB and KT approaches will be compared.

## 2. Computational Method

When the alternative KB approximation is applied to the  $\pi^*$  temporary anion states of the series of substituted benzenes, the electron affinity is expressed as

$$EA \approx -\varepsilon_{VMO} - \frac{\Delta_{xc}}{2} \quad (3)$$

where  $\varepsilon_{VMO}$  denotes the Kohn–Sham one-electron eigenvalue associated with the  $\pi^*$  virtual molecular orbital (VMO). It follows from eq 1 that

$$EA \approx -(\varepsilon_{VMO} + \varepsilon_{HOMO} + IP) \quad (4)$$

Notice that eq 4 was derived in ref 14 using  $\varepsilon_{LUMO}$  instead of  $\varepsilon_{VMO}$ . The vertical attachment energy, i.e. the negative of EA, can then be represented as

$$AE \approx \varepsilon_{VMO} + \varepsilon_{HOMO} + IP \quad (5)$$

The virtual orbital energy associated with the temporary anion state is also known as AE. The AE obtained from KB approach in eq 5 will be denoted as  $\varepsilon_{VMO}^{KB}$ .

In this study, the stabilization method is employed to distinguish the  $\pi^*$  orbital solutions from the virtual ODC solutions. Three different Gaussian-type basis sets are employed for our calculations. (1) The 6-31+G(d)+ $\alpha p_1$  basis set is formed by augmenting the 6-31+G(d) basis set with the diffuse  $p_1$  function multiplied by a scale factor,  $\alpha$  (denoted by  $\alpha p_1$ ), on the C, N, O, and F atoms. The  $p_1$  functions have the exponents of 0.0146, 0.0213, 0.02817, and 0.03587 for the C, N, O, and F atoms, respectively. (2) The 6-31+G(d)+ $\alpha(p_1, p_2)$  basis set is formed by augmenting the 6-31+G(d)+ $\alpha p_1$  basis set with the

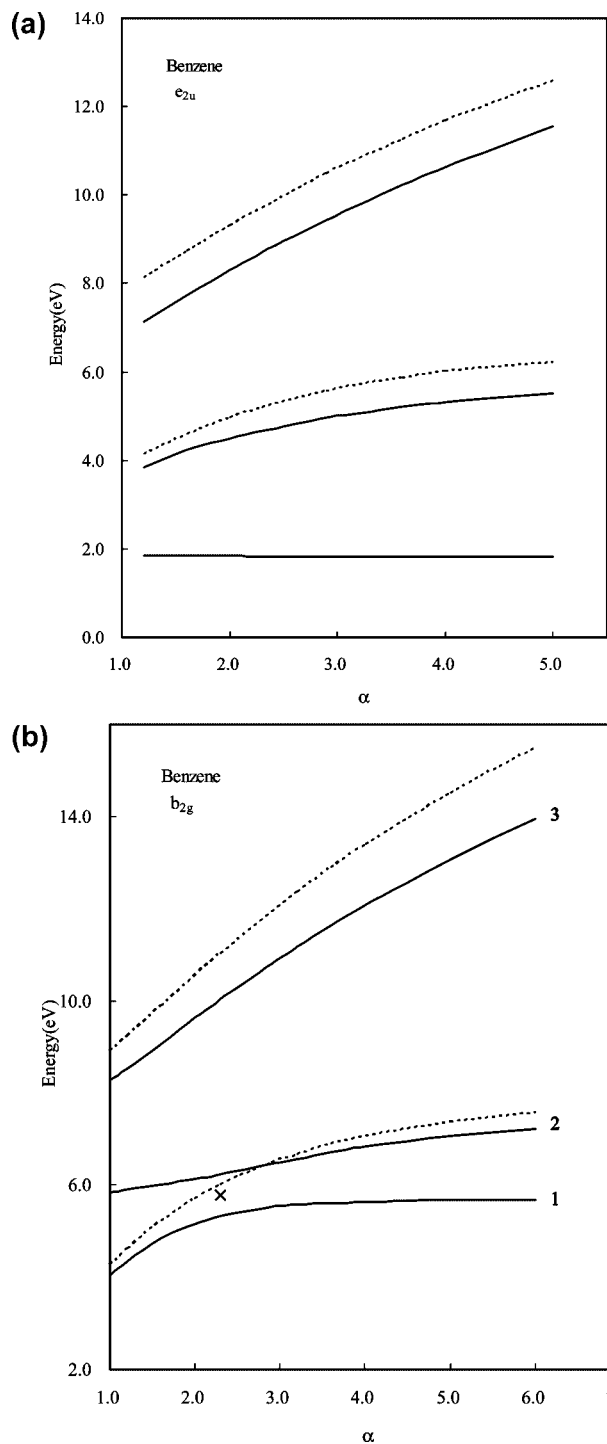


**Figure 2.** Stabilization graphs for benzene. Energies of (a)  $e_{2u}$  and (b)  $b_{2g}$  virtual orbitals (represented by the solid curves) and the free electron (represented by the dashed curves) as a function of  $\alpha$  using the 6-31+G(d)+ $\alpha p_1$  basis set. The location of  $\alpha_{xc}$  is marked with  $\times$ .

$\alpha p_2$  diffuse function. The  $p_2$  functions have the exponents of 0.00487, 0.0071, 0.00939, and 0.01196 for the C, N, O, and F atoms, respectively. (3) The aug-cc-pvdz+ $\alpha p_3$  basis set is formed by augmenting the aug-cc-pvdz basis set with the  $\alpha p_3$  diffuse function. The  $p_3$  functions have the exponents of 0.01347, 0.01870, 0.02285, and 0.02834 for the C, N, O, and F atoms, respectively. The inclusion of additional diffuse s functions or d polarization functions is found to be unimportant for the energies of  $\pi^*$  orbitals. As  $\alpha$  increases, the ODC

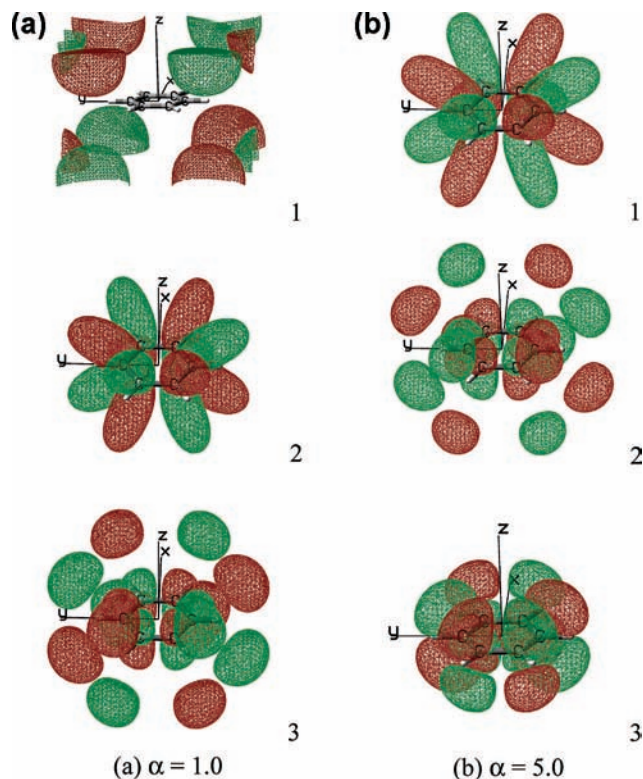


**Figure 3.** Plots of the first three  $b_{2g}$  virtual orbitals for benzene at (a)  $\alpha = 1.0$  and (b)  $\alpha = 5.0$ . The isosurface values chosen for all the MO plots are 0.02 except for the first  $b_{2g}$  virtual orbital that is 0.01 at  $\alpha = 1.0$ . These values are chosen so that surface building will not be out of range.

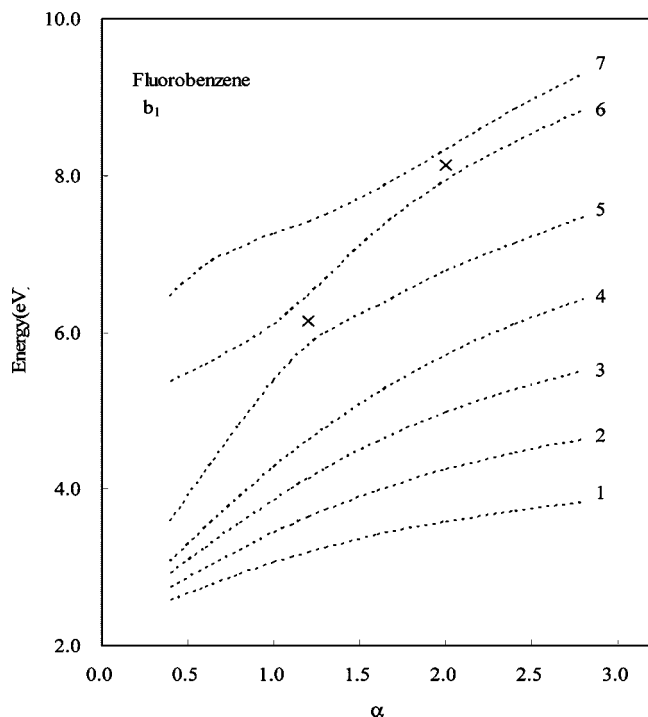


**Figure 4.** Energies of  $b_1$  virtual orbitals of fluorobenzene as a function of  $\alpha$  for a free electron in the absence of potentials using the 6-31+G(d)+ $\alpha p_1$  basis set.

solutions may approach the  $\pi^*$  orbital solutions in energy and lead to avoided crossing between the two types of solutions.

The stabilization graphs are obtained by plotting the calculated energies ( $\epsilon_{VMO}^{KB}$ ) as a function of the scale factor  $\alpha$ . The energy

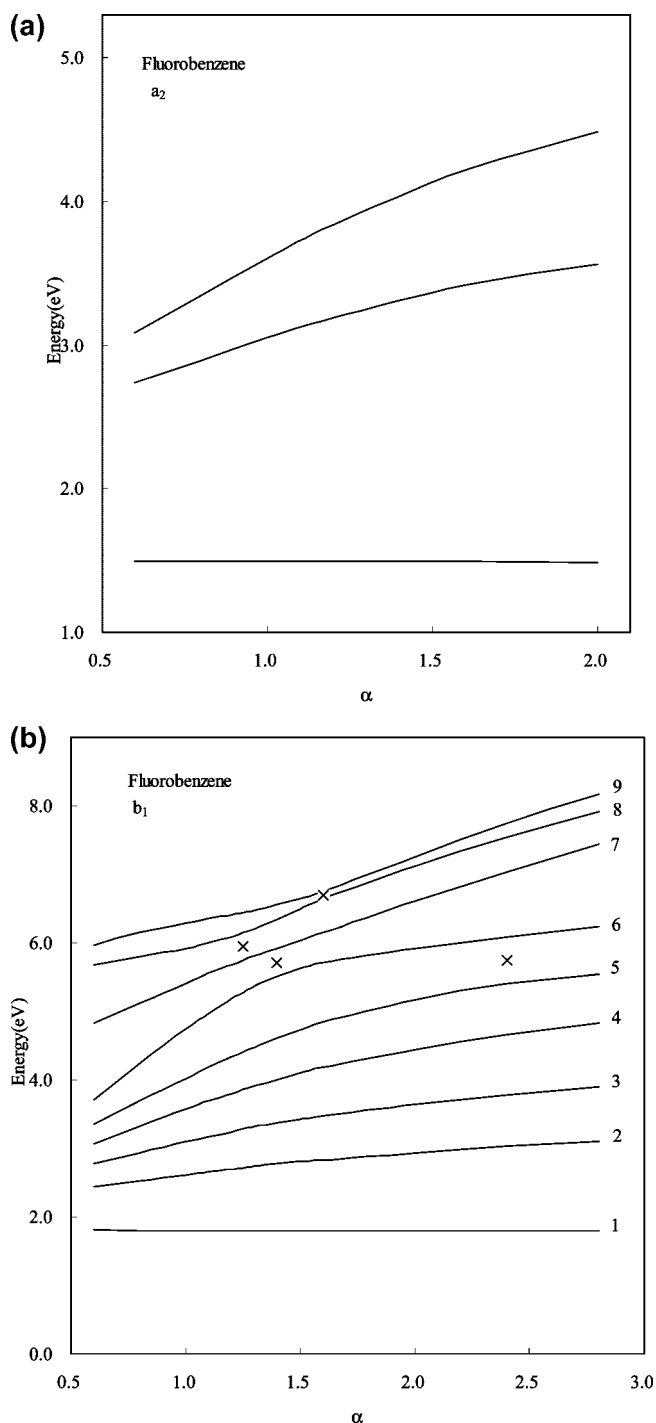


**Figure 5.** Stabilization graphs for fluorobenzene. Energies of (a)  $a_2$  and (b)  $b_1$  virtual orbitals as a function of  $\alpha$  using the 6-31+G(d)+ $\alpha p_1$  basis set. The locations of  $\alpha_{ac}$  are marked with  $\times$ .

of the stabilized  $\pi^*$  orbital is taken as the mean value of the two eigenvalues involved in the avoided crossing at their point of closest approach,  $\alpha_{ac}$ , if the avoided crossing occurs between temporary anion and ODC solution.<sup>31,32</sup>

In this paper, we will first use the mostly used B3LYP hybrid method involving the three-parameter Becke exchange functional<sup>33</sup> and a Lee–Yang–Parr correlation functional.<sup>34</sup> It combines a generalized gradient approximation (GGA) term with a fraction of orbital exchange. Then, the PBEPBE method<sup>35</sup> using pure GGA functional as in the works of Tozer and co-workers is also employed. All calculations are performed using the Gaussian 03 program.<sup>36</sup> The geometries used for the

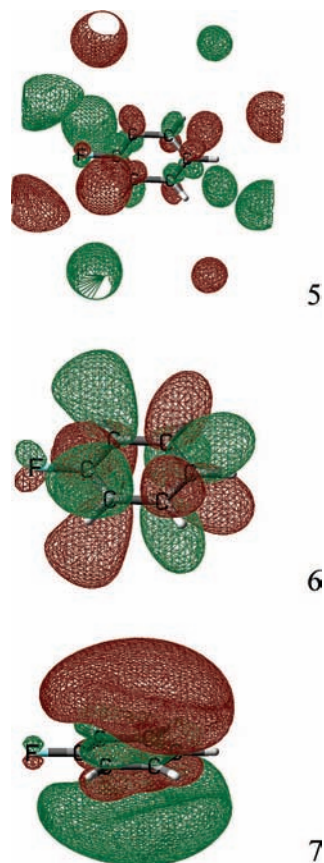


**Figure 6.** Plots of the fifth, sixth, and seventh  $b_1$  virtual orbitals at  $\alpha = 2.0$  for fluorobenzene. The isosurface values are chosen to be 0.02 for all the MO plots. These values are chosen so that surface building will not be out of range.

calculations are taken from experiment.<sup>37–40</sup> An exception is the HOC angle of phenol, which is taken to be  $180^\circ$  to allow the calculations to exploit  $C_{2v}$  symmetry. Our symmetry in the labeling of the orbitals is based on the  $z$  axis that is perpendicular to the plane of molecules.

### 3. Results and Discussion

Figure 1 shows the energies of the discrete continuum (DC)<sup>20–23</sup> solutions as a function of scale factor  $\alpha$  for the  $e_{2u}$  and  $b_{2g}$  virtual orbitals of benzene using the  $6-31+G(d)+\alpha p_1$  basis set. The energies of the DC solutions are obtained by solving the Kohn–Sham equation for a free electron in the absence of any potential. With this basis set, there are two  $e_{2u}$  and two  $b_{2g}$  DC solutions that lie below 15.0 eV for  $1 < \alpha < 5.0$ .

We perform S-KB calculations on the  $\pi^*$  orbitals to distinguish them from the ODC solutions. The stabilization graphs of the energies as a function of  $\alpha$  for the  $e_{2u}$  and  $b_{2g}$  virtual states of benzene and the free electron using the  $6-31+G(d)+\alpha p_1$  basis set are shown in Figure 2, parts a and b, respectively. There are two types of energies for  $\pi^*$  virtual orbitals in the S-KB calculations. One is the  $\pi^*$  orbital solution and the other the ODC virtual orbital solution. The  $\pi^*$  orbital solution and the ODC solutions are readily distinguished by examining how their energies vary with  $\alpha$ . As shown in Figure 2a, the first solution that remains stabilized with  $\alpha$  is the  $e_{2u}$   $\pi^*$  orbital solution, and the stabilized energy value is 1.84 eV. The next two solutions that are appreciably higher in energies than the resonance solution correspond to the ODC solutions. In general, the energies of ODC lie below that of the DC.

For the  $b_{2g}$  virtual states of benzene in Figure 2b, the third solution that increases with increasing  $\alpha$  is the ODC solution. The first and second solutions undergo an avoided crossing at  $\alpha_{ac}$ . The energy of the  $b_{2g}$   $\pi^*$  orbital is 5.78 eV at  $\alpha_{ac} = 2.3$ . The nature of the first and second solutions can be examined as follows. Just to the left of the avoided crossing ( $\alpha < 2.3$ ), the first solution that contains predominantly extra diffuse function character is from the ODC solution, while the second solution that contains largely  $\pi^*$  orbital character is from the  $\pi^*$  orbital. On the other hand, to the right of the avoided crossing ( $\alpha > 2.3$ ), the first solution is from the  $\pi^*$  orbital, while the second solution is from the ODC solution. To illustrate the aforementioned observation, three  $b_{2g}$  virtual orbitals for  $\alpha = 1.0 (< \alpha_{ac})$  and  $\alpha = 5.0 (> \alpha_{ac})$  are displayed. Notice that the first virtual orbitals are all similar to each other for  $\alpha > \alpha_{ac}$ . Here, the value  $\alpha = 5.0$  can be arbitrarily chosen as long as it is greater than  $\alpha_{ac}$ . As shown in Figure 3a, the second virtual orbital of  $\alpha = 1.0$  corresponds to  $\pi^*$  orbital. Two other virtual orbitals correspond to ODC solutions. Similarly in Figure 3b, the first virtual orbital of  $\alpha = 5.0$  is also from  $\pi^*$  orbital and resembles the second virtual orbital in Figure 3a.

Figure 4 shows the energies of the DC solutions as a function of scale factor  $\alpha$  for the  $b_1$  virtual orbitals of fluorobenzene using the  $6-31+G(d)+\alpha p_1$  basis set. For energies smaller than 10.0 eV and  $\alpha$  smaller than 3.0, the fifth, sixth, and seventh DC solutions are coupled with each other. The avoided crossings resulting from the couplings between the fifth and sixth DC solutions and between the sixth and seventh DC solutions are located at  $\alpha_{ac}(5,6) = 1.2$  and  $\alpha_{ac}(6,7) = 2.0$ , respectively.

The stabilization graphs of energies for the  $a_2$  and  $b_1$   $\pi^*$  virtual orbitals of fluorobenzene using the  $6-31+G(d)+\alpha p_1$  basis set are shown in Figure 5, parts a and b, respectively. By examining the energies, as indicated in Figure 5a, the first solution that remains almost constant is the first  $a_2$   $\pi^*$  (denoted as  $2a_2$ ) orbital solution, and the obtained stabilized energy value is 1.81 eV. The next two solutions having appreciably higher energies than the  $2a_2$  correspond to the ODC solutions. Similarly, the first solution in Figure 5b that remains almost constant is the first  $b_1$   $\pi^*$  (denoted as  $4b_1$ ) orbital solution, and the stabilized energy value of the  $4b_1$  orbital is 1.50 eV. As illustrated in Figure 5b, the second, third, and fourth solutions, which increase with increasing  $\alpha$ , are the first, second, and third ODC solutions. Four avoided crossings regions are found in Figure 5b. They are from the couplings between the fifth and sixth solutions, the sixth and seventh solutions, the seventh and eighth solutions, and the eighth and ninth solutions. The locations of them are at  $\alpha_{ac}(5,6) = 2.4$ ,  $\alpha_{ac}(6,7) = 1.4$ ,  $\alpha_{ac}(7,8) = 1.3$ , and  $\alpha_{ac}(8,9) = 1.6$ , respectively. The nature of the fifth to ninth solutions is examined as follows. As an example, Figure 6 displays the fifth, sixth, and seventh  $b_1$  virtual orbitals of fluorobenzene for  $\alpha = 2.0$ . As indicated in this figure, the sixth  $b_1$  virtual orbital is from the second  $b_1$   $\pi^*$  (denoted as  $5b_1$ ) orbital, and the other two virtual orbitals containing extra diffuse function character are from ODC solutions. On the basis of Figures 4 and 5b and the analysis of the nature of virtual orbitals, the eighth solution for  $\alpha < 1.3$ , the sixth solution for  $1.4 < \alpha < 2.4$ , and the fifth solution for  $\alpha > 2.4$  are mainly from the  $5b_1$   $\pi^*$  orbital solution. The fifth solution for  $\alpha < 2.4$  and the sixth solution for  $\alpha > 2.4$  are from the fourth ODC solution. The sixth solution for  $\alpha < 1.4$  and the seventh solution for  $\alpha > 1.4$  correspond to the fifth ODC solution. The seventh solution for  $\alpha < 1.3$  and the eighth solution for  $\alpha > 1.3$  are from the sixth ODC solution. Finally, the ninth solution is from the seventh ODC solution. The energies of the  $\pi^*$  orbital can be extracted from each



**TABLE 1: Calculated<sup>a</sup> and Corrected<sup>b</sup> AEs (eV) of Benzene, Pyridine, Phenol, and Fluorobenzene via S-KB Approach**

compd	orbital	S-KB <sup>c</sup>						$X\alpha^d$ B	ESKT <sup>e</sup>		Expt <sup>f/g</sup>
		6-31+G(d)+ $\alpha p_1$		6-31+G(d)+ $\alpha(p_1+p_2)$		aug-cc-pvdz+ $\alpha p_3$			6-31+G(d)+ $\alpha p_1$		
		B3LYP	PBEPBE	B3LYP	PBEPBE	B3LYP	PBEPBE		HF		
benzene	b <sub>2g</sub>	5.78 (5.06)	5.95 (4.98)	5.82 (5.11)	5.92 (4.92)	5.62 (5.03)	5.50 (4.85)	5.62 (4.92)	6.61 (4.66)	4.82	
	e <sub>2u</sub>	1.84 (1.12)	2.09 (1.12)	1.83 (1.12)	2.12 (1.12)	1.71 (1.12)	1.77 (1.12)	1.85 (1.12)	3.07 (1.12)		
pyridine	4b <sub>1</sub>	5.71 (4.99)	5.71 (4.74)	5.78 (5.07)	5.70 (4.70)	5.59 (5.00)	5.59 (4.94)	5.51 (4.81)	6.10 (4.15)	4.58	
	2a <sub>2</sub>	1.81 (1.09)	2.00 (1.03)	1.80 (1.09)	2.00 (1.00)	1.74 (1.15)	1.94 (1.29)	1.66 (0.96)	2.95 (1.00)		1.20
	3b <sub>1</sub>	1.46 (0.74)	1.65 (0.68)	1.42 (0.71)	1.64 (0.64)	1.38 (0.79)	1.59 (0.94)	1.14 (0.44)	2.43 (0.48)		
phenol	5b <sub>1</sub>	6.26 (5.54)	5.94 (4.97)	6.40 (5.69)	6.15 (5.15)	5.97 (5.38)	5.66 (5.01)	5.85 (5.15)	6.49 (4.54)	4.92	
	4b <sub>1</sub>	2.12 (1.40)	2.20 (1.23)	2.10 (1.39)	2.19 (1.19)	1.98 (1.39)	2.07 (1.42)	2.06 (1.36)	3.70 (1.75)		1.73
	2a <sub>2</sub>	1.82 (1.10)	1.85 (0.88)	1.78 (1.07)	1.84 (0.84)	1.68 (1.09)	1.72 (1.07)	1.63 (0.93)	2.96 (1.01)		
fluorobenzene	5b <sub>1</sub>	5.72 (5.00)	5.65 (4.68)	5.87 (5.16)	5.60 (4.60)	5.49 (4.90)	5.42 (4.77)	5.97 (5.27)	6.41 (4.46)	4.80	
	4b <sub>1</sub>	1.81 (1.09)	1.88 (0.91)	1.80 (1.09)	1.86 (0.86)	1.70 (1.11)	1.78 (1.13)	2.25 (1.55)	3.05 (1.10)		1.48
	2a <sub>2</sub>	1.50 (0.78)	1.52 (0.55)	1.46 (0.75)	1.53 (0.53)	1.38 (0.79)	1.45 (0.80)	1.52 (0.82)	2.59 (0.64)		
$d^h/eV$		0.79	0.84	0.81	0.85	0.64	0.67	0.72	1.75		

<sup>a</sup> The energies of the HOMO ( $\epsilon_{\text{HOMO}}$ ) in eq 5 are calculated for each value of  $\alpha$  even though the  $\epsilon_{\text{HOMO}}$  values do not change very much. <sup>b</sup> The corrected values (shown in parentheses) were obtained by subtracting the amount needed to bring the calculated AEs into agreement with experimental values for the  ${}^2E_{2u}$  anion state of benzene. <sup>c</sup> Present study. <sup>d</sup> From ref 28. <sup>e</sup> From ref 29. <sup>f</sup> The experimental AEs of benzene and fluorobenzene are obtained from refs 46 and 47, respectively. The values for pyridine and phenol are from ref 45. <sup>g</sup> The error in these values is within  $\pm 0.1$  eV. (refs 28, 48). <sup>h</sup>  $d$  denotes the mean error relative to experimental data.

**TABLE 2: Calculated and Corrected<sup>a</sup> AEs (eV) of Benzene, Pyridine, Phenol, and Fluorobenzene via KT Approach**

compd	orbital	6-31+G(d)		aug-cc-pvdz	
		B3LYP	PBEPBE	B3LYP	PBEPBE
benzene	b <sub>2g</sub>	3.48 (4.97)	2.68 (4.88)	3.33 (4.93)	2.53 (4.84)
	e <sub>2u</sub>	-0.37 (1.12)	-1.08 (1.12)	-0.48 (1.12)	-1.19 (1.12)
pyridine	4b <sub>1</sub>	1.54 (3.03)	1.25 (3.45)	1.30 (2.90)	1.04 (3.35)
	2a <sub>2</sub>	-0.69 (0.80)	-1.43 (0.77)	-0.76 (0.84)	-1.50 (0.81)
	3b <sub>1</sub>	-1.04 (0.45)	-1.77 (0.43)	-1.11 (0.49)	-1.85 (0.46)
phenol	5b <sub>1</sub>	1.91 (3.40)	1.58 (3.78)	1.63 (3.23)	1.33 (3.64)
	4b <sub>1</sub>	0.05 (1.54)	-0.64 (1.56)	-0.09 (1.51)	-0.77 (1.54)
	2a <sub>2</sub>	-0.30 (1.19)	-0.99 (1.21)	-0.43 (1.17)	-1.11 (1.20)
fluorobenzene	5b <sub>1</sub>	1.68 (3.17)	1.37 (3.57)	1.43 (3.03)	1.15 (3.46)
	4b <sub>1</sub>	-0.40 (1.09)	-1.09 (1.11)	-0.49 (1.11)	-1.17 (1.14)
	2a <sub>2</sub>	-0.72 (0.77)	-1.41 (0.79)	-0.81 (0.79)	-1.49 (0.82)
$d^b/eV$		2.00	2.61	2.15	2.74

<sup>a</sup> The corrected values (shown in parentheses) were obtained by subtracting the amount needed to bring the calculated AEs into agreement with experimental values for the  ${}^2E_{2u}$  anion state of benzene. <sup>b</sup>  $d$  denotes the mean error relative to experimental data.

avoided crossing region. The energy values obtained from the avoided crossings are 5.74 eV at  $\alpha_{ac}(5,6)$ , 5.72 eV at  $\alpha_{ac}(6,7)$ , 5.95 eV at  $\alpha_{ac}(7,8)$ , and 6.69 eV at  $\alpha_{ac}(8,9)$ , respectively. According to the aforementioned observation, only the avoided

crossings at  $\alpha_{ac}(5,6)$ ,  $\alpha_{ac}(6,7)$ , and  $\alpha_{ac}(7,8)$  are due to the coupling between 5b<sub>1</sub>  $\pi^*$  orbital and the fourth, fifth, and sixth ODC solutions. On the other hand, the avoided crossing at  $\alpha_{ac}(8,9)$  is due to the coupling between the sixth and seventh ODC solutions.<sup>41</sup> Therefore, it is important to exclude the result obtained from  $\alpha_{ac}(8,9)$ . The lowest value from each set of energy values will be defined as the energy of the  $\pi^*$  orbital.<sup>29</sup> Thus, the energy of the 5b<sub>1</sub> orbital is 5.72 eV.

The stabilization graphs of energies for both phenol and pyridine are similar to those of fluorobenzene. As to the S-KB/6-31+G+ $\alpha p_1$  calculations on phenol, the stabilized energy values of 2a<sub>2</sub> and 4b<sub>1</sub> orbitals are 1.82 and 2.12 eV, respectively. The avoided crossings at  $\alpha_{ac} = 1.6$  and 2.4 are due to the coupling between the 5b<sub>1</sub> orbital solution and ODC solutions. The energy values of 5b<sub>1</sub> orbital are 6.32 eV at  $\alpha_{ac} = 2.4$  and 6.26 eV at  $\alpha_{ac} = 1.6$ . Accordingly, the energy of the 5b<sub>1</sub> orbital is 6.26 eV. For the S-KB/6-31+G+ $\alpha p_1$  calculations on pyridine, the stabilized energy values of 2a<sub>2</sub> and 3b<sub>1</sub> orbitals are 1.81 and 1.46 eV, respectively. The energy values of 4b<sub>1</sub> orbital obtained are 5.78 eV at  $\alpha_{ac} = 1.0$  and 5.71 eV at  $\alpha_{ac} = 1.6$ . Therefore, the energy of the 4b<sub>1</sub> orbital is 5.71 eV.<sup>42</sup> Notice that the avoided crossings will not be observed in the stabilization graphs for the  ${}^2E_{2u}$   $\pi^*$  state of benzene,  ${}^2A_2$ , and the first  ${}^2B_1$   $\pi^*$  states of the substituted benzenes when more diffuse p functions are added.<sup>43</sup>

The results of various S-KB and KT calculations of AEs are summarized in Tables 1 and 2, respectively. To compare with experimental results, "corrected" AEs are also included in the tables. The corrected values are obtained by subtracting the amount  $b$  from the calculated AE values to bring the  ${}^2E_{2u}$  anion state of benzene into agreement with the experimental value. For instance, in B3LYP/6-31+G(d)+ $\alpha p_1$  calculations,  $b$  is 0.72.

First, we discuss the results obtained from the B3LYP method. Table 1 shows that the AEs obtained from the 6-31+G(d)+ $\alpha p_1$  and 6-31+G(d)+ $\alpha(p_1+p_2)$  basis sets are close to each other. When the basis set is sufficient to span the space, there is almost no change in the AEs results. The inclusion of the diffuse  $p_2$  function proves to be relatively unimportant. The mean errors for AEs are 0.79 and 0.81 eV for the 6-31+G(d)+ $\alpha p_1$  and 6-31+G(d)+ $\alpha(p_1+p_2)$  basis sets, respectively. When the larger aug-cc-pvdz+ $\alpha p_3$  basis set is used, the AEs obtained are closer to experimental values. The mean error for AEs relative to the experimental data is reduced to 0.64 eV. However, the mean error is about 1.75 eV when the Hartree–Fock exponent-stabilized Koopmans' theorem (ESKT) method<sup>29</sup> is used. In Table 2, the mean errors for AEs are 2.00 and 2.15 eV for the 6-31+G(d) and aug-cc-pvdz basis sets, respectively. For the third anion state (which falls in the 4–5 eV range) of the substituted benzenes, the mean error is around 3.18 eV. According to Tables 1 and 2, the S-KB approach yields an improvement in the prediction of the absolute energies of  $\pi^*$  states over KT and ESKT approaches.

The  ${}^2E_{2u}$  anion of benzene splits into  ${}^2A_2$  and the first  ${}^2B_1$   $\pi^*$  state in the substituted benzenes. When using the S-KB B3LYP/aug-cc-pvdz+ $\alpha p_3$  method, the error for  ${}^2E_{2u}/{}^2B_{2g}$  splitting of benzene is 0.21 eV, and the average error for the  ${}^2A_2$ /first  ${}^2B_1$  and  ${}^2A_2$ /second  ${}^2B_1$  splittings of substituted benzenes is 0.29 eV. According to Table 2, none of the KT calculations account quantitatively for the relative AEs between the  ${}^2A_2$  and second  ${}^2B_1$  anion states. The average error for the  ${}^2A_2$ /second  ${}^2B_1$  splittings of substituted benzenes is 1.63 eV when using the aug-cc-pvdz basis set. Hence, Tables 1 and 2 demonstrate that the S-KB approach generates more accurate relative AEs than those of the KT. The inherent experimental errors for the ETS structures for the  ${}^2B_{2g}$  state of benzene, the third anion states of the substituted benzenes, and the second anion states of pyridine and fluorobenzene could be as large as 0.1 eV. The errors associated with determination of the resonance energies from the stabilization graphs could also be as large as 0.1 eV.<sup>28,48</sup> Consequently, the S-KB approach can yield reasonable predictions of the relative energies of  $\pi^*$  states when using the flexible sizes of basis sets.

Next, we compare the results obtained from the B3LYP and PBEPBE methods. For all the molecules, the  $\epsilon_{\text{HOMO}}^{\text{PBEPBE}}$  values lie above  $\epsilon_{\text{HOMO}}^{\text{B3LYP}}$ . All  $\text{AE}^{\text{PBEPBE}}$  values lie above  $\text{AE}^{\text{B3LYP}}$  values except for the  ${}^2B_{2g}$  state of benzene and the third anion states of the substituted benzenes. As shown in Table 1, the mean errors for AEs obtained from the PBEPBE method are slightly larger than those obtained from the B3LYP method ( $\sim 0.04$  eV). Similarly, for all the molecules, the  $\epsilon_{\text{VMO}}^{\text{PBEPBE}}$  values lie below  $\epsilon_{\text{VMO}}^{\text{B3LYP}}$ . Hence, the mean errors for AEs obtained from the PBEPBE method (2.61 and 2.74 eV) are larger than those obtained from the B3LYP method (2.00 and 2.15 eV) when using the KT approach (Table 2). As to the relative AEs, both S-KB<sup>PBEPBE</sup> and ESKT approaches yield better results than the S-KB<sup>B3LYP</sup>, as indicated in Table 1. When using the PBEPBE/aug-cc-pvdz+ $\alpha p_3$  method, the error for  ${}^2E_{2u}/{}^2B_{2g}$  splitting of benzene is 0.03 eV, and the average error for the  ${}^2A_2$ /first  ${}^2B_1$  and  ${}^2A_2$ /second  ${}^2B_1$  splittings of substituted benzenes is 0.20 eV. The error for  ${}^2E_{2u}/{}^2B_{2g}$  splitting of benzene and the average error for the  ${}^2A_2$ /first  ${}^2B_1$  and  ${}^2A_2$ /second  ${}^2B_1$  splittings of substituted benzenes are both 0.16 eV when the ESKT method is employed. To sum up, the B3LYP method generally yields slightly better absolute AEs, yet slightly worse relative AEs as compared to the PBEPBE method. One possible reason for this

discrepancy is due to the different Coulomb contributions at large electron-molecule distance between these two methods.

According to Table 1, the AEs of S-KB/aug-cc-pvdz+ $\alpha p_3$  are close to those obtained from the multiple scattering  $X\alpha$  self-consistent-field (MS- $X\alpha$ -SCF) method using basis set B of similar size and with similar virial ratio.<sup>28</sup> The  $X\alpha$  theory can be regarded as a special case of DFT. In the  $X\alpha$ /stabilization method, the AEs are calculated by Slater's transition state method<sup>44</sup> with half an electron added to an empty orbital. However, the success of the  $X\alpha$  calculations for the series of substituted benzenes is due in part to the fact that  $\sigma/\pi$  orbital mixing is not important. One main drawback in multiple-scattering  $X\alpha$  method is that it does not treat the  $\sigma$  and  $\pi$  orbitals on an equal footing when using the muffin-tin approximation (MTA). For systems in which  $\sigma/\pi$  mixing is important, the  $X\alpha$  method may generate unreliable results for relative AEs. Moreover, the EAs obtained from the  $X\alpha$  method are also found to be quite sensitive to the sphere overlap used for MTA. The modern DFT method has been used widely and proved to be more successful than the  $X\alpha$  method in many systems. Therefore, the S-KB method is more useful in studying the AEs of temporary anion states than the  $X\alpha$ /stabilization method.

#### 4. Conclusion

The energies of  $\pi^*$  anion states obtained from the S-KB method have been systematically studied in benzene and substituted benzenes by using the DFT method. The present investigation has demonstrated that the S-KB method is able to yield an improvement in predicting the absolute energies of  $\pi^*$  states for substituted benzenes over KT and ESKT approaches. The key factors to the superiority of our approach are (1) the adoption of a stabilization method that can allow us to distinguish the  $\pi^*$  virtual orbitals coming from either the  $\pi^*$  resonance or ODC solutions and (2) the use of KB approximation instead of KT. It is believed that the S-KB method should be very useful in determining the energies of temporary anion states for aromatic systems.

**Acknowledgment.** We would like to thank the reviewers for valuable comments during the revision process and the National Center for High-Performance Computing for the computational resources provided. This work was supported by National Science Council of Republic of China.

#### References and Notes

- (1) Simons, J. *J. Phys. Chem. A* **2008**, *112*, 6401.
- (2) Domcke, W.; Mundel, C.; Cederbaum, L. S. *Comments At. Mol. Phys.* **1987**, *20*, 293.
- (3) Paddon-Row, M. N.; Wong, S. S. *Chem. Phys. Lett.* **1990**, *167*, 432.
- (4) Jordan, K. D.; Paddon-Row, M. N. *J. Phys. Chem.* **1992**, *96*, 1188.
- (5) Paddon-Row, M. N.; Jordan, K. D. *J. Am. Chem. Soc.* **1993**, *115*, 2952.
- (6) Jordan, K. D.; Paddon-Row, M. N. *Chem. Rev.* **1992**, *92*, 395.
- (7) Paddon-Row, M. N.; Shephard, M. J.; Jordan, K. D. *J. Phys. Chem.* **1993**, *97*, 1743.
- (8) Mikkelsen, K. V.; Ratner, M. D. *Chem. Rev.* **1987**, *87*, 113.
- (9) Newton, M. D. *Chem. Rev.* **1991**, *91*, 767.
- (10) Sanche, L.; Schulz, G. J. *Phys. Rev.* **1972**, *5*, 1672.
- (11) Jordan, K. D.; Burrow, P. D. *Chem. Res.* **1987**, *87*, 557.
- (12) Koopmans, T. *Physica* **1934**, *1*, 104.
- (13) Kohn, W.; Sham, L. J. *Phys. Rev. A* **1965**, *140*, 1133.
- (14) Tozer, D. J.; De Prof, F. *J. Phys. Chem. A* **2005**, *109*, 8923.
- (15) Tozer, D. J.; De Prof, F. *J. Chem. Phys.* **2007**, *127*, 034108.
- (16) De Prof, F.; Sablon, N.; Tozer, D. J.; Geerlings, P. *Faraday Discuss.* **2007**, *135*, 151.
- (17) Sablon, N.; De Prof, F.; Geerlings, P.; Tozer, D. J. *J. Phys. Chem. Chem. Phys.* **2007**, *9*, 5880.

- (18) Teale, A. M.; De Proft, F.; Tozer, D. J. *J. Chem. Phys.* **2008**, *129*, 044110.
- (19) Hajgató, B.; Deleuze, M. S.; Tozer, D. J.; De Proft, F. *J. Chem. Phys.* **2008**, *129*, 084308.
- (20) Falcetta, M. F.; Jordan, K. D. *J. Phys. Chem.* **1990**, *94*, 5666.
- (21) Falcetta, M. F.; Jordan, K. D. *J. Am. Chem. Soc.* **1991**, *113*, 2903.
- (22) Burrow, P. D.; Howard, A. E.; Johnston, A. R.; Jordan, K. D. *J. Phys. Chem.* **1992**, *96*, 7570.
- (23) Juang, C.-Y.; Chao, J. S.-Y. *J. Phys. Chem.* **1994**, *98*, 13506.
- (24) Hazi, A. H.; Taylor, H. S. *Phys. Rev.* **1970**, *A1*, 1109.
- (25) Taylor, H. S. *Adv. Chem. Phys.* **1970**, *18*, 91.
- (26) Fels, M. F.; Hazi, A. U. *Phys. Rev.* **1972**, *A5*, 1236.
- (27) Taylor, H. S.; Hazi, A. U. *Phys. Rev.* **1976**, *A14*, 2071.
- (28) Chao, J. S.-Y.; Jordan, K. D. *J. Phys. Chem.* **1987**, *91*, 5578 (Note: Chao, J. S.-Y. is Cheng, Hsiu-Yao, who has adopted her maiden name as the corresponding author in this paper.).
- (29) Chen, C.-S.; Feng, T.-H.; Chao, J. S.-Y. *J. Phys. Chem.* **1995**, *99*, 8629.
- (30) Wei, Y.-H.; Cheng, H.-Y. *J. Phys. Chem. A* **1998**, *102*, 3560.
- (31) We use the simplest "midpoint method" adopted by Burrow et al.<sup>22</sup> The performance of the midpoint method is reasonable when compared with those obtained from the more rigorous analytic continuation method (ref 19 in ref 23).
- (32) Various methods have been proposed to estimate resonance state energies and lifetimes from the avoided crossings between the eigenvalues of the stabilization graphs. (a) Simons, J. *J. Chem. Phys.* **1981**, *75*, 2465. (b) Frey, R. F.; Simons, J. *J. Chem. Phys.* **1986**, *84*, 4462. (c) Chao, J. S.-Y.; Falcetta, M. F.; Jordan, K. D. *J. Chem. Phys.* **1990**, *93*, 1125. (d) Chao, J. S.-Y. *Chem. Phys. Lett.* **1991**, *179*, 169.
- (33) Becke, A. D. *J. Chem. Phys.* **1993**, *98*, 5648.
- (34) Lee, C.; Yang, W.; Parr, R. G. *Phys. Rev. B* **1988**, *37*, 785.
- (35) Perdew, J. P.; Burke, K.; Ernzerhof, M. *Phys. Rev. Lett.* **1996**, *77*, 3865.
- (36) Frisch, M. J.; Trucks, G. W.; Schlegel, H. B.; Scuseria, G. E.; Robb, M. A.; Cheeseman, J. R.; Montgomery, J. A., Jr.; Vreven, T.; Kudin, K. N.; Burant, J. C.; Millam, J. M.; Iyengar, S. S.; Tomasi, J.; Barone, V.; Mennucci, B.; Cossi, M.; Scalmani, G.; Rega, N.; Petersson, G. A.; Nakatsuji, H.; Hada, M.; Ehara, M.; Toyota, K.; Fukuda, R.; Hasegawa, J.; Ishida, M.; Nakajima, T.; Honda, Y.; Kitao, O.; Nakai, H.; Klene, M.; Li, X.; Knox, J. E.; Hratchian, H. P.; Cross, J. B.; Adamo, C.; Jaramillo, J.; Gomperts, R.; Stratmann, R. E.; Yazyev, O.; Austin, A. J.; Cammi, R.; Pomelli, C.; Ochterski, J. W.; Ayala, P. Y.; Morokuma, K.; Voth, G. A.; Salvador, P.; Dannenberg, J. J.; Zakrzewski, V. G.; Dapprich, S.; Daniels, A. D.; Strain, M. C.; Farkas, O.; Malick, D. K.; Rabuck, A. D.; Raghavachari, K.; Foresman, J. B.; Ortiz, J. V.; Cui, Q.; Baboul, A. G.; Clifford, S.; Cioslowski, J.; Stefanov, B. B.; Liu, G.; Liashenko, A.; Piskorz, P.; Komaromi, I.; Martin, R. L.; Fox, D. J.; Keith, T.; Al-Laham, M. A.; Peng, C. Y.; Nanayakkara, A.; Challacombe, M.; Gill, P. M. W.; Johnson, B.; Chen, W.; Wong, M. W.; Gonzalez, C.; Pople, J. A. *Gaussian 03, revision C.02*; Gaussian, Inc.: Wallingford CT, 2004.
- (37) Burrow, P. D.; Modelli, A.; Guerra, M.; Jordan, K. D. *Chem. Phys. Lett.* **1985**, *118*, 328.
- (38) Bak, B.; Hansen-Nygaard, L.; Rastrup-Andersen, J. *J. Mol. Spectrosc.* **1958**, *2*, 361.
- (39) Nygaard, L.; Bojesen, I.; Pederson, T.; Rastrup-Andersen, J. *J. Mol. Struct.* **1968**, *2*, 209.
- (40) Pederson, T.; Larsen, M. W.; Nygaard, L. *J. Mol. Struct.* **1969**, *4*, 59.
- (41) When the basis set is insufficient to span the space, free electron solutions could be undergoing avoided crossings. When more diffuse functions are included, some of the avoided crossings between the free electron solutions may be removed. For instance, when an additional  $\alpha p_2$  diffuse function is added to the 6-31+G(d)+ $\alpha p_1$  basis set, the avoided crossing around  $\alpha_{cc}(8,9)$  is removed.
- (42) We have estimated the resonance widths from the avoided crossings using the method proposed in ref 32. The obtained widths for the  $2B_{2g}$  state of benzene,  $4b_1$  state of pyridine,  $5b_1$  state of phenol, and  $5b_1$  state of fluorobenzene are 0.52, 0.11, 0.26, and 0.46 eV when using the B3LYP/6-31+G+ $\alpha p_1$  method and the values are 0.52, 0.16, 0.19, and 0.27 eV when using the PBEPBE/6-31+G+ $\alpha p_1$  method, respectively. These values, except the value for benzene, are not very accurate as compared to the experimental data (0.6 eV for benzene,  $\sim 1$  eV for the substituted benzenes). One possible explanation for the inaccuracy is that the correlation and relaxation effects are not fully considered by the KB approximation. As to other  $\pi^*$  anion states, the avoided crossings are not found in the stabilization graphs.
- (43) It is because the calculated VMO eigenvalues ( $\epsilon_{VMO}$ ) for the  $\pi^*$  states are negative for all  $\alpha$ . However, the VMO eigenvalues for a free electron are always positive. Hence, the energies of ODC solutions are higher than those of the  $\pi^*$  states. Consequently, no avoided crossings will be found in the stabilization graphs.
- (44) Gopinathan, M. S. *J. Phys. B* **1979**, *12*, 521, and references therein.
- (45) Jordan, K. D.; Burrow, P. D. *Acc. Chem. Res.* **1978**, *11*, 341.
- (46) Burrow, P. D.; Michejda, J. A.; Jordan, K. D. *J. Chem. Phys.* **1987**, *86* (1), 9.
- (47) Olthoff, J. K.; Tossell, J. A.; Moore, J. H. *J. Chem. Phys.* **1985**, *83* (11), 5627.
- (48) Jordan, K. D.; Michejda, J. A.; Burrow, P. D. *J. Am. Chem. Soc.* **1978**, *98*, 7189.